The effect of controlled release of celecoxib on the gene expression and biochemical composition of extracellular matrix in a canine model of IVD degeneration.

S.J. Kamphuijs

3576825

Internship Orthopaedics Research Group

Faculty Veterinary Medicine, Utrecht University

Start date: June the 6th 2016

Email: S.J.Kamphuijs@students.uu.nl

Supervisors: A.R. Tellegen (A.R.Tellegen@uu.nl) & M.A. Tryfonidou (M.A.Tryfonidou@uu.nl)

Universiteit Utrecht

Content

Abstract

Introduction. Intervertebral disc degeneration (IVDD) is a common spinal disorder in both humans and dogs. It is characterized by symptoms ranging from mild back or neck pain to severe neurological deficits. Current therapies to relieve clinical symptoms due to IVDD are often unsatisfactory, since they only provide a palliative treatment and they do not treat the degenerated disc. Previous research showed a similarity in etiopathogenesis of IVDD in humans and dogs, thereby making the dog an excellent model for treatment research. The aim of the present study was to evaluate the effect of two doses of intradiscal controlled released celecoxib (a selective COX-2 inhibitor), on artificially induced IVDD in Beagle dogs. The effect of celecoxib was determined through analysis of biochemical content (GAG, collagen and DNA) and gene expression for specific biomarkers for degeneration and regeneration.

Material & Methods. In six male Beagle dogs IVDD was induced and after four weeks of degeneration, magnetic resonance (MR) imaging was performed and two concentrations (0,01 and 0,3 mg/40 µl) of celecoxib loaded polyester amide polymers microspheres (PEAMs) were injected. This created four conditions: low and high dose of celecoxib, untreated IVDs and IVDs injected with empty PEAMs. After three months dogs were again MR imaged and euthanized for further evaluation. Spinal segments were dissected and IVDs were cut into quarters before cryosections were made, whereafter nucleus pulposus (NP) tissue and annulus fibrosus (AF) tissue were split for further laboratory analysis. The NP samples were evaluated for both biochemical analyses of GAG, collagen and DNA content and gene expression, and the AF samples were only taken into account for biochemical analysis (GAG, collagen and DNA).

Results. Results of the NP samples showed that both low and high doses of celecoxib increased the GAG and collagen content compared with the empty PEAMs condition. Also, the collagen content was increased in the low dose celecoxib condition compared with the untreated condition. For the AF samples only an increased content of GAG was found when high dose of celecoxib was compared with the untreated condition. Overall, results showed a tendency that low dose of celecoxib resulted in higher content of GAG and collagen compared to the other conditions. When GAG and collagen were corrected for DNA there were no differences found in the NP samples. Only in the AF samples the DNA content seemed to be less in both celecoxib conditions compared with the empty PEAMs condition. No results were acquired from the qPCR for gene expression analysis.

Discussion and conclusion. The higher content of GAG and collagen in both celecoxib conditions in NP and AF samples compared with both control conditions allow the assumption that there is a regenerative effect of celecoxib on IVDD independent of the dose. More specific, results showed a tendency that the IVDs injected with a low dose celecoxib scored higher in GAG and collagen content compared with high dose of celecoxib. An explanation may come from the inhibitory effect on proliferation and induction of cell cycle arrest effects of celecoxib and other COX-2 inhibitors, a characteristic that is gratefully used in anti-cancer treatments. However, no significant differences were found between low and high dose of celecoxib. More laboratory tests must be done to acquire an optimal, safe and effective concentration of celecoxib to be injected and will be effective in degenerated IVDs. Eventually, intradiscal injected PEAMs loaded with celecoxib might be a promising long-term, curative and minimally invasive treatment in canine patients with IVDD and associated clinical symptoms.

Introduction

Clinical importance. Lower back pain is a common spinal disorder in both humans and dogs with a lifetime prevalence of 70% in the human population worldwide. It is one of the major causes for loss of workdays and it leads to very high medical costs annually due to clinical signs ranging from only mild back pain up to neurological deficits [1,15]. The clinical signs and etiopathogenesis are similar for both humans and dogs and can be the result of degeneration of the intervertebral discs (IVDs) located between the vertebral bodies of the spine [1].

Intervertebral disc degeneration. The intervertebral discs stabilise the spine and make it possible for the spine to move in many different directions without causing damage. The intervertebral disc is composed of a central nucleus pulposus (NP), this is a mucoid, translucent, bean-shaped structure composed mainly of water (80%). In the healthy IVD the main cell type of the NP are notochordal cells (NCs) [2,17]. The extracellular matrix of the NP is made up by a complex network of two negatively charged structures (proteoglycans and hyaluronic acid) interwoven with collagen fibres (mainly type II), that are produced by the NCs [17]. Proteoglycans consist of a core protein with one or more covalently bound glycosaminoglycan (GAG) chains. Aggrecan is the major proteoglycan found in the IVD [2]. Water is strongly attracted to the negatively charged complexes and helps to absorb the compression during axial movement. The NP is surrounded by the annulus fibrosus (AF) which gives protection and prevents the NP from damage. The AF is composed of a network of fibrinous lamellae and consists of 60% water. The transition zone (TZ) is the inner part of the AF and is composed of mainly collagen type II and a mixed population of fibrocytes and chondrocyte-like cells, whereas the outer part of the AF is mainly collagen type I and fibrocyte-like cells (figure 1A, [2]).

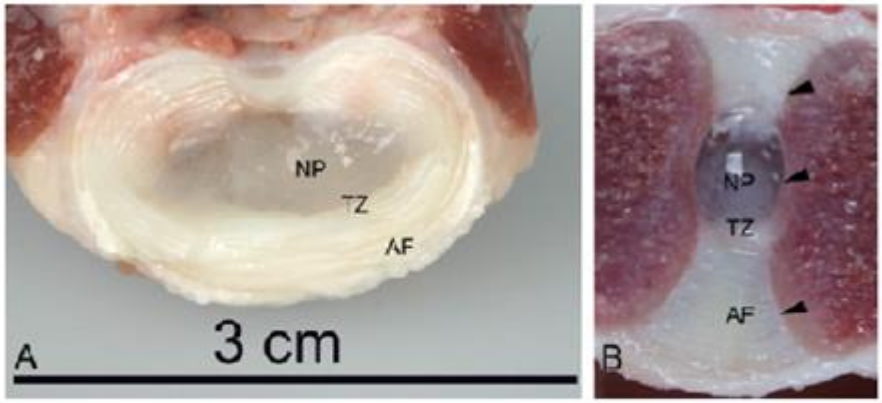

Fig. 1. Transverse (A) and sagittal (B) sections through a L5-L6 intervertebral disc of a mature non-chondrosytrophic dog, showing the nucleus pulposus (NP), transition zone (TZ), annulus fibrosus (AF), and endplates (arrowheads).

Reprinted from Bergknut *et al.* (2013), *The Veterinary Journal,* vol. 195.3, p. 283.[2]

The sagittal cross-section shows the endplates, which form the cranial and caudal borders of the IVD (figure 1B, arrowheads [2]). The endplates (EP) are very similar to that of articular cartilage and are composed of mainly water with a matrix of proteoglycans, hyaluronic acid and collagen type II. The EP is very important for the IVD, because it regulates the transport of small molecules into and from the IVD. The IVD itself is avascular and depends on the EP and the outer most part of the AF for blood supply and nutrients [2]. During embryogenesis the notochord forms the cranial-caudal axis of the body and later give rise to the AF, TZ, endplates and vertebral bodies of the spine. The notochord condenses in the centre of the AF to form the NP [17,28]. In cervical IVDs the AF consists of 13-32 layers of collagen laminae, similar to the 15-30 distinct layers reported for lumbar IVDs [20].

Degeneration of the IVD is a complex process and many different causes for degeneration and lower back pain are previously discussed for dogs [2]. Most studies about IVD degeneration (IVDD) make a distinction between chondrodystrophic (CD) breeds and non-chondrodystrophic (NCD) breeds based on their physical appearance, like chondrodysplasia [3,17]. Chondrodysplasia is a type of skeletal dysplasia characterized by abnormal endochondral ossification of the long bones, resulting in a disproportionate short stature with the typical bow-shaped extremities [1,17,18]. This trait is strongly linked with IVDD, which is thought to be of polygenetic origin [3,17]. The pathogenesis of IVD degeneration is similar for

both groups of dogs, but the origination differs for age of onset, type of herniation it may lead to and the frequency and location of spine segments involved. IVD degeneration is thought to be more spontaneously in young to middle-aged CD dogs due to genetic predilection and may lead to more type I herniation in the cervical and thoracolumbar segments [1,3,5]. IVD degeneration in CD breeds is often called chondroid metaplasia [28]. In NCD dogs IVD degeneration is often called fibrous metaplasia and is thought to be more due to trauma and wear-and-tear in older dogs and may lead to more type II herniation in the lumbosacral segments [1,3,5,28]. IVD diseases are more common in CD breeds than in NCD breeds and show a prevalence of 3,5% before the age of 12 in the total dog population. The morbidity of IVD diseases is about 34% in the total dog population, with a prevalence of 20% in most CD breeds and up to a prevalence of more than 50% in some high-risk NCD breeds [22].

Degeneration is characterized by an alteration in cells and extracellular matrix of the IVD and is normally a natural process that occurs with aging [28]. The alterations are little described in dogs, but more extensively in humans and because previous research has shown similarities in the etiopathogenesis of IVD degeneration in humans and dogs, results found in human studies may be extrapolated to the situation in both CD and NCD dogs [1]. As can be seen in figure 2 [2], many factors may initiate, affect or accelerate (green arrows) the IVD degeneration and functional failure of the extracellular matrix. Functional and structural failure of the matrix has effect on the enzyme activity and biochemical composition of the IVD [2,15]. During IVD degeneration, a decrease in proteoglycan content is seen, together with a decrease in synthesis of collagen type II fibres. At the same time, denaturation of collagen type II fibres occurs and synthesis of collagen type I fibres is upregulated in the extracellular matrix of the NP [15]. The main cell type of the NP is also changing. In CD breeds, the main cell type of the NP shifts from notochordal cells (NC) to chondrocyte-like cells (CLCs) at about 1 year of age (figure 3 [2,17,37]), but NCs remain the main cell type until middle/old age in NCD breeds [17]. Also the lamellae of the AF become disrupted and both tissues decrease in size [15]. The fibrils of the outer AF become coarser and more susceptible to injury [15,17].

Typical notochordal markers are the proteins brachyury (T) and cytokeratins (CKs), which will be less expressed

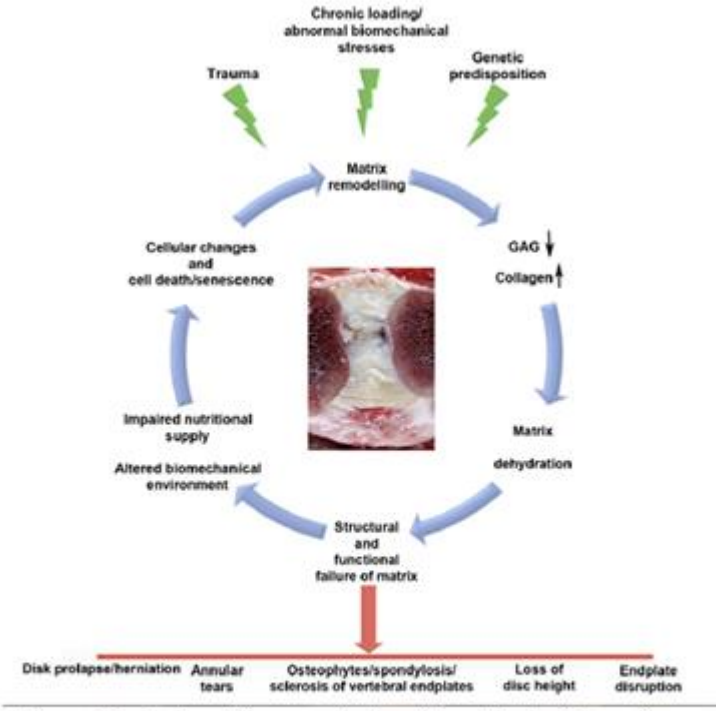

Fig 2. Generalized, schematic representation of the pathophysiology of intervertebral disc degeneration showing the vicious circle of repeated failure and inadequate repair.

Reprinted from: Bergknut *et al.* (2013), *The Veterinary Journal*, vol. 195, p 286.[2]

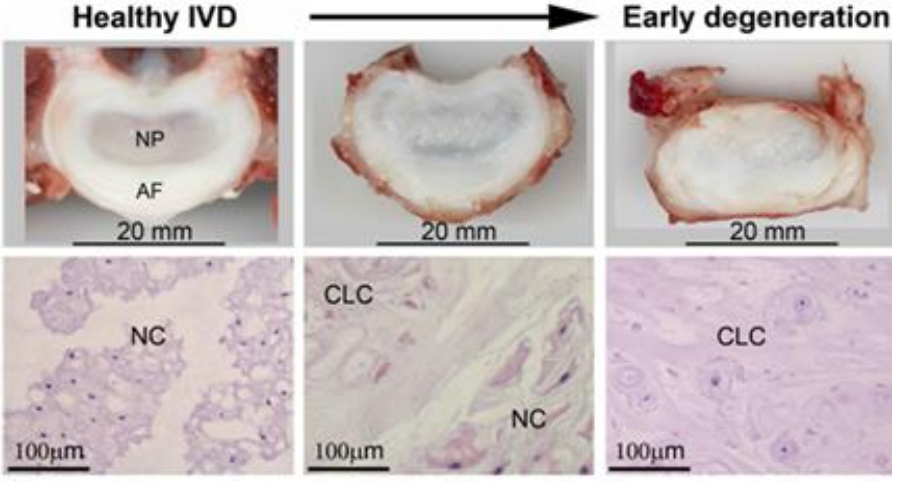

Fig 3. Fases of degeneration from healthy to early degeneration. Macroscopic and microscopic images of different fases of degenerated IVDs. Left: a healthy IVD, with a clear nucleus pulposus (NP), annulus fibrosus (AF) and transitional zone (TZ). The main cell type is notochordal cells (NC). Middle and right: during disc degeneration the distinction between NP and AF becomes less clear and the main cell type shifts to chondrocyte-like cells .

Reprinted from: Bach *et al.* (2014), *BMC Veterinary Research*, vol 4 10:3 p. 2[17]

during IVDD. Furthermore, in healthy discs only the outer third of the AF is innervated [28], but due to high levels of a neuropeptide called nerve growth factor (NGF) during degeneration, the nerve endings extend into the deeper layers of the AF and even into the NP. Stimulation through mechanical or inflammatory stimuli can cause a nociceptive response leading to discogenic pain sensation [11,15].

Taken together, the matrix becomes more rigid and loses the hydrostatic properties, making the IVD more prone to structural changes (figure 2 red arrow [2]). Furthermore, the structural and functional failure of the matrix leads to an alteration in the biomechanical environment of the IVD with an impaired flow of nutrients and fluid in and out of the IVD. Due to the inadequate nutritional supply to the damaged matrix, IVD cells become impaired to repair the matrix with cellular changes and cell death with necrosis as a consequence [1]. This will further deteriorate the health and regeneration of the IVD and stimulate the ongoing remodelling of the matrix, illustrated by the vicious circle of figure 2 (blue arrows [1,2]).

Molecular factors relevant for pathological processes. During the pathological process of IVD disease, many changes in molecular and enzymatic activity are seen and responsible for the process of degeneration and inflammation of the IVD [10]. The quality of the extracellular matrix is important for strength and movement of a healthy IVD and is secured by a balanced activity level of anabolic and katabolic processes [6,8]. Important proteins are aggrecan (ACAN) and collagen (COLs), which are broken down by, respectively, matrix metalloproteinases (MMPs) and a disintegrin and metalloproteinase with thrombospondin motifs (ADAMTs). Another important enzymes are tissue inhibitor of metalloproteinases (TIMPs) which regulate MMPs and ADAMTs [8]. Furthermore, the GAG content decreases due to less deposition during IVDD and the confluence of less GAG and more denatured collagen type II content leads to a starch and rigid IVD matrix which is more prone to trauma [2,17,25,28]. Various pro-inflammatory molecules are also involved, such as interleukins (ILs), tumour necrosis factor-α (TNFα) and nerve growth factor (NGF) [6,10,11]. Prostaglandin E_2 (PGE_2) is a common prostanoid and essential for physiological processes, but it also plays an important regulatory role in pathological processes like IVDD [6,20]. In the NP, PGE_2 inhibits the synthesis of proteoglycan and thus negatively affects the integrity of the extracellular matrix during IVDD [6]. PGE_2 is synthesized in two steps. First, arachidonic acids are converted into prostaglandin H_2 (PGH_2) by two enzymes, cyclooxygenase 1 and 2 (COX-1 and COX-2). Then, PGH_2 is isomerized to PGE_2 by the enzyme prostaglandin E synthase (PGES 1 and 2) (figure 4 [20]) [6].

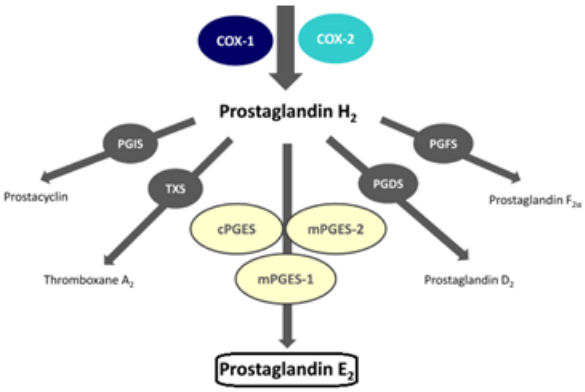

Fig. 4. Synthesis of Prostaglandine E_2 by the enzymes $PGES_1$ and $PGES_2$ from Prostaglandin H_2. Arachidonis acid is first converted into Prostaglandin H_2 by cyclooxygenase 1 (COX-1) and cyclooxygenase 2 (COX-2).

Reprinted from Sharan *et al.* (2013), Basic Science of Spinal Diseases, chapter 6, p 44 [20].

The process of apoptosis is also part of IVD degeneration. Apoptosis or programmed cell-death is a physiological process and part of homeostasis, but when tissue is inflamed or disturbed the process may get excessive. Because apoptosis during IVDD is known to follow the mitochondrial apoptosis pathway [29], there are two proteins of interest which are expressed: the anti-apoptotic B-cell lymphoma (BCL2) and the pro-apoptotic BCL-associated X (BAX) [9,29].

Possible treatments. Current treatments of IVD degeneration and lower back pain in dogs consist of cage rest, physiotherapy, pain medication or surgical intervention [5,28]. However, cage rest, physiotherapy and surgical intervention are unsatisfactory as they do not reverse the process of disc degeneration and each modality has their own disadvantages. Cage rest and exercise restriction for 2 to 5 weeks has a very big influence on the quality of the dog's life and its interaction with the owner. Furthermore, there is no certainty that the ruptured AF will heal and that clinical signs will improve [28]. Surgical treatment is costly due to MR imaging prior to surgery and the intervention itself, also a long period of post-operative

care is needed. Medication such as analgesics, muscle relaxants and anti-inflammatory drugs are frequently prescribed by veterinarians, but oral medication will not always obtain functional concentrations at the location of interest, here the IVD and are of unknown benefit [28]. Long-time medication is not favourable due to side effects and possible loss of owner's compliance [4,28].

Anti-inflammatory therapy. Targeting the inflammation process is one of the key treatment strategies of chronic lower back pain and IVD degeneration [6]. Discogenic pain is caused by a confluence of deeper innervation, inflammation and mechanical hypermobility of the IVD [11]. Anti-inflammatory therapy may prevent deeper sensory nerve ingrowth of IVDs and thus prevent sensitization of sensory nerve fibres innervating the IVD [11,28]. Anti-inflammatory drugs also suppress the production of inflammatory cytokines and diminish the process of degeneration [1,6]. If this process is suppressed, less collagenases will be produced which otherwise will lead to hypermobility and thus more pain [11]. There are different types of anti-inflammatory drugs and one type are the non-steroidal anti-inflammatory drugs (NSAIDs). NSAIDs are a frequently chosen treatment option for chronic lower back pain. NSAIDs prevent the formation of prostaglandins through the inhibition of the enzyme cyclooxygenase (COX) as can be seen in figure 4 [20]. More specifically, most NSAIDs inhibit both COX-1, which is expressed in nearly all body tissues and of importance for physiological processes and COX-2, which is expressed in very low levels in normal tissues but is rapidly and excessively induced in inflamed tissue, for instance during IVDD [16]. Medications that specifically inhibit only COX-2 have less negative influence on COX-1 and its associated physiological processes. Another advantage is that COX-2 is known to produce PGE_2, thus when COX-2 is inhibited, PGE_2 will also be less expressed as can be seen in figure 4 [20].

Celecoxib. Celecoxib is such a specific COX-2 inhibitor and decreases the production of prostaglandins and thereby decreases the process of inflammation [2,16]. Celecoxib is a drug registered for humans and is prescribed to ease pain due to rheumatoid arthritis, osteoarthritis and spondylitis ankylopoetica [12]. Further, celecoxib is known to downregulate the activity of the Wnt-signalling pathway, which is composed of a group of signal transduction proteins from the cell membrane to the nucleus for gene transcription [13]. In healthy cells the activity of this pathway is strictly regulated, but in inflamed tissue the signal transduction of the Wnt-signalling pathway is upregulated. Axin-2, c-Myc and Cyclin-D1 are three target genes involved in this pathway and their expression (and because of that the expression of Wnt-signalling pathway) will be reduced due to celecoxib [13]. Taken together, celecoxib will not only decrease inflammation and degeneration and therefore interrupt the vicious circle of IVD degeneration, but celecoxib can also prevent deeper sensory innervation of IVDs and thus provide an analgesic effect [10]. More knowledge about tissue concentration of celecoxibot is needed in both humans and dogs.

Sustained release formulations. Previous studies reported a positive effect of systematically COX-2 inhibitors on IVD degeneration and diminished the sensitisation of lower back pain [6]. However, the widespread application of NSAIDs in general is impeded by severe side effects, such as cardiotoxicity and gastro-intestinal problems like gastric ulceration and renal damage [15,16]. Therefore, gastro-protective drugs that counteract the damaging effects are usually added, but a combination therapy brings new problems of pharmacokinetics, toxicity and owner's compliance [4,16,28]. New methods of administration are developed and especially the local intradiscal injection is of interest [4,6]. Research has been done and results show that NSAIDs may also be effectively introduced through intradiscal injections into the IVD [4]. However, NSAIDs would achieve only short term clinical effects as they are chemical instable and quickly metabolised [4,11]. New insights about slow-released medication encounter these implications, making intradiscal injections a minimal invasive technique to introduce bioactive substances like NSAIDS to the location of interest [6]. Locally injected slow-release medication from biodegradable substances can acquire higher loading dose and long-term delivery with therapeutically effective local concentrations, without causing adverse side effects [4,6]. Even more, compared with every day oral administration of drugs, a long acting injection will also improve owner's compliance. An in vitro study examined the biocompatibility and effect of controlled released celecoxib from such a biodegradable

substance, here of interest was thermoreversible poly-N-isopropylacylamide MgFe-layered double hydroxide (pNIPAAM MgFe-LDH) hydrogel on canine IVD cells in a pro-inflammatory environment with TNF-α [6]. The results showed a degeneration of the hydrogel and an increase of [celecoxib] over time and an inhibition of PGE_2 production for 28 days, leading to the conclusion that slow-released celecoxib can inhibit PGE_2 induced inflammation over a longer period of time [6].

Another type of slow-release biomaterials are polyester amide polymers (PEAs) which are biodegradable by endogenous enzymes. PEAs are synthetic, amino-acid-based polymers, build up from three different building blocks (figure 5 [40]) combining ester and amide groups in the polymer chain [40]. This creates amphiphilicity and eases interactions with proteins, increases biodegradability and modifications with bioactive molecules and drugs, like celecoxib [4,40]. Furthermore, an important feature is that the good thermal and mechanical properties of PEAs make degradation through surface erosion mechanism possible [40]. PEAs are first synthesized [41], and in the first step of creating the microparticles, the relevant drug can be added. The PEA microspheres (PEAMs) are further prepared via the emulsion solvent-evaporation technique [40]. Research has shown that PEAs did not cause cytotoxicity or inflammation in mouse fibroblast cells, macrophages or retinal cells [4,40]. In vitro release studies of PEAMs loaded with dexamethason showed a controlled release of the drug for a period up to 90 days, and a kinetic ocular model showed an expected in vivo drug concentration even 90 days after injection [40]. In rabbits, PEAs showed only a slight foreign body response after intramuscular injection in vivo [4], no reaction was seen when PEAMs were injected extra- and intraocular in mice [40]. This leads to the conclusion that PEAs have a good cytocompatibility and biocompatibility and are considered as a save slow-release delivery system [4]. Furthermore, PEAMs injected into healthy IVDs did not cause any complications over a follow-up period of 6 months [4].

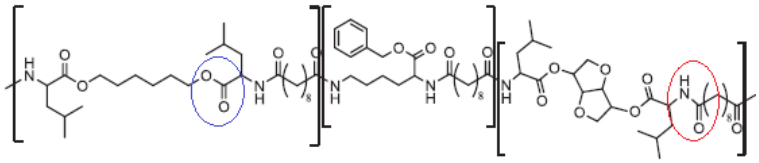

Fig 5. Structure of PEA. Created from three building blocks, randomly distributed over the polymer chain. Each block contains ester (blue circle) and amide groups (red circle).

Reprinted from: Andrés *et al.* (2015), *Journal of Controlled Release, vol 211, p 105-117* [40].

Purpose of the study. The purpose of this study is to examine the effect of two doses of locally placed slow released celecoxib incorporated in PEAMs through intradiscal injection on the process of IVD degeneration in the dog. Also, more knowledge about tissue concentration over time should be acquired. Eventually, the aim is to develop a long-acting, safe and effective treatment for dogs with chronic pain due to IVD degeneration by declining the process of degeneration and relieving neurogenic pain. Furthermore, the treatment may be also used in humans with lower back pain and maybe even as a treatment for chronic pain due to lesions in the cartilage of the knee.

Hypothesis. The associated hypotheses are:
H0: There will be no difference in gene expression for different biomarkers of degeneration between the inducted IVDs injected with low concentration celecoxib, high concentration celecoxib and both controls. Also, there will be no influence of celecoxib on the biochemical contents GAG and collagen corrected for DNA.

H1: There will be a difference in gene expression for different biomarkers of degeneration between inducted IVDs injected with low concentration celecoxib, high concentration celecoxib and controls. The expectation is that discs injected with a high concentration celecoxib will have increased concentrations of anabolic and anti-inflammatory biomarkers and lower concentrations of catabolic, inflammatory and apoptosis biomarkers compared with the control IVDs (degenerated IVDs injected with empty PEAMs and untreated IVDs) and the low concentration celecoxib injected IVDs. Also, there will be an effect of celecoxib on biochemical contents, specifically upregulation of GAGs, and more collagen type II synthesis compared with the controls. It is thought that the higher dose of celecoxib will lead to a bigger response.

Material & Methods

Subjects.

Dogs. Six male Beagles of 18 months old were used. IVD degeneration was induced alternately in 5 segments of the lumbar spine by NP aspiration according through the method of Hiyama *et al.* (2008) [23]. Briefly, the segments were carefully exposed and punctured in the centre of the disc with an 18-gauge needle through the AF into the NP. Next, some tissue was aspirated using a 10-ml syringe to induce intervertebral disc degeneration [23]. Four weeks after induction magnetic resonance imaging was done to assess IVD degeneration. One dog had 8 instead of 7 lumbar segments, making a total of 55 IVDs for further analyses.

IVD induction and treatment. The dogs were divided into two groups (triamcinolone (TAA) or celecoxib (CXB)). Segments were alternately induced with IVD degeneration and intradiscal drug injections were given in accordance to the following model:

Normal scheme		7345 induction		7345 injection	
T12-T13	Sham	T12-T13	Sham	T12-T13	Sham
T13-L1	None	T13-L1	None	T13-L1	None
L1-L2	Tx	L1-L2	Tx	L1-L2	Tx
L2-L3	None	L2-L3	None	L2-L3	None
L3-L4	Tx	L3-L4	Tx	L3-L4	Tx
L4-L5	None	L4-L5	None	L4-L5	None
L5-L6	Tx	L5-L6	Tx	L5-L6	None
L6-L7	none	L6-L7	None	L6-L7	Tx
L7-S1	Tx	L7-L8	None	L7-L8	None
		L8-S1	Tx	L8-S1	Tx

Dog	Level					
TAA	**T12-T13**	**L1-L2**	**L3-L4**	**L5-L6**	**L6-L7**	**L7-S1**
7269	empty PEAMs	LD	LD	HD		HD
2645	empty PEAMs	LD	HD	HD		LD
5466	empty PEAMs	HD	LD	HD		LD
CXB	**T12-T13**	**L1-L2**	**L3-L4**	**L5-L6**	**L6-L7**	**L7-S1**
7345	empty PEAMs	HD	LD		LD	HD
7362	empty PEAMs	HD	LD	HD		LD
9054	empty PEAMs	HD	HD	LD		LD

Table 1. Distribution of dogs per condition. Above: Left column: normal induction/injection scheme per dog. Middle and right columns: dog 7345 had 8 instead of 7 lumbar segments. Therefore, one more segment was left with no induction and treatment (L7-L8). The injection L5-L6 and L6-L7 were mingled. Tx = treatment. Sham = injection with 0,9% NaCl and empty PEAMs. None = no induction/no injection. Below: Three dogs were treated with triamcinolone (TAA) in two concentrations (LD = 0,0084 mg/40 µl; HD = 0,84 mg/40 µl) and another three dogs were injected with celecoxib (CXB) in two concentrations (LD = 0,01 mg/40 µl; HD = 0,3 mg/40 µl). PEAMs = polyester amide polymer microspheres.

The micro particles with low concentration triamcinolone contained 0,0084 mg/40 µl and the high concentration was 0,84 mg/40 µl. The micro particles with low celecoxib contained 0,01 mg/40 µl and the high concentration contained 0,3 mg/40 µl celecoxib. The control injection was 0,9% NaCl and empty PEAMs. For this specific part of the study only celecoxib was of interest.

Follow up. The dogs were followed for four months and IVD degeneration was determined with MR imaging before the dogs were euthanized. The spines were cut into parts per IVD and frozen for further

research (-80 °C). All segments were examined for the degree of IVD degeneration and therefor the effect of celecoxib on the process of degeneration.

Sample collection. Cryosections were cut at 60 µm thickness with a cryotome. NP and AF were divided with a scalpel and placed into two different collection tubes with different buffers: the complete lysis M buffer (Roche Diagnostics Nederland B.V., Almere, The Netherlands) for biochemical analysis and the Exiqon kit lysis buffer (Exiqon, Vadbaek, Denmark) for gene expression. After this, the collection tubes with the samples were stored at -80 °C. Also, some tissue was cut separately for MSI to evaluation if remnants of drug were still present in the injected IVDs.

Gene expression.

Tissue lyser & RNA isolation. The samples were defrosted and 200 µl of lysis buffer (Exiqon, Vadbaek, Denmark) and a metal bead were added to the vial, then the samples were lysed in a TissueLyser II (Qiagen, Venlo, The Netherlands) for 4 minutes at 20 Hz. Next, RNA isolation was performed according to the manufacturers guideline, here briefly explained: each sample was centrifuged for three minutes at maximal speed (13.200g). The supernatant was transferred to a new vial and 500 µl of 70% ethanol (7ml:2,6ml 96% ethanol and RNase free water) was added and mixed, whereafter the content was placed onto the column to catch RNA. The column was then centrifuged for 1 minute at maximal speed, flow-through was thrown away. Then the column was washed with 400 µl Wash Solution (1ml:2,3ml of Wash Buffer and 96% ethanol) and centrifuged for 2 minutes at maximal speed. The collection tubes with the flow-through were discarded. Next, 100 µl of DNase was placed on the membrane of the column and centrifuged for 2 minutes at minimal speed (80g) and the flow-through was transferred back onto the membrane and incubated for 15 minutes. Thereafter, the column was washed twice with 400 µl Wash Buffer and centrifuged for 1 minute at maximal speed. Next the column was centrifuged for 2 minutes at maximal speed and the collection tubes were discarded. As a last step, 30 µl of Elution buffer was placed directly on the membrane of the column and de samples were centrifuged for 2 minutes at minimal speed (0.8g), followed by 1 minute at maximal speed before stored at -70 °C before cDNA synthesis was performed. The same steps were separately performed for the 55 NP and AF samples.

RNA quantification & cDNA synthesis. After RNA isolation two randomly chosen NP samples were used for RNA quantification with a NanoDrop 1000 spectrophotometer (Isogen Life Science, Ijsselstein, The Netherlands). Thereafter, cDNA was synthesized using the iScript cDNA Synthesis Kit (Bio-Rad, Veenendaal, The Netherlands). Furthermore, cDNA was diluted 10x (10 µl cDNA and 90 µl MQ). Standard line was made taking 8 µl from every 10x diluted cDNA sample and taken together to obtain S1, this was further diluted with 1:4 with MQ up to S7. S8 contained only MQ. Then 40 µl of 10x diluted cDNA was further diluted with 160 µl MQ to make 50x diluted cDNA. This was used to perform qPCR. The 10x diluted cDNA was stored in freezer and standards and 50x diluted in the fridge.

Qubit RNA assay & Bioanalyzer. A Qubit RNA fluorometer assay (Invitrogen, Paisley, UK) was performed to quantify the content of RNA per NP sample. Briefly, Qubit Working Solution was prepared by diluting 1 µl Qubit reagent in 199 µl Qubit buffer. Standard line was made by diluting 10 µl of standard 1 and standard 2 separate in 190 µl Working Solution. Next, for each sample thin-wall clear 0,5 ml PCR tubes were filled with 190 µl of Working Solution and 10 µl of each sample was added. Of some samples there was not enough RNA left, so then 5 µl of sample was diluted in 195 µl Working Solution. Each sample was vortexed and placed in the Qubit 2.0 Fluorometer and readings were taken. Results are shown in Additional files table 1.

Second, a bioanalysis was performed from eleven randomly chosen NP samples to assess the quality and integrity of the extracted RNA using a Bioanalyzer (Aligent Technologies, Amstelveen, the Netherlands), according to associated protocol of Aligent RNA 6000 Pico Assay, here briefly described. Gel was previously prepared by centrifuging 550 µl of Gel Matrix at 1500 g for 10 minutes. Then, 65 µl was taken and mixed with 1 µl of vortexed Pico Dye Concentrate at room temperature and 9 µl the Gel-Dye mix was pipetted into the well marked G of a new RNA 6000 Pico chip. A plunger positioned

at 1 ml was pressed until it was held by the clip and after exactly 30 seconds the clip was released and allowed to return to the 1 ml position. The plunger was removed and 9 µl of Gel-Dye mix was added into two other wells marked G. Then, 9 µl of RNA 6000 Pico Conditioning Solution was placed into the CS marked well and 5 µl of RNA 6000 Pico Marker was pipetted in all 11 sample wells and in the ladder well. Loading of the chip was done with 1 µl of Pico ladder into the associated well and 1 µl of each denaturalised (2 minutes at 70 °C) sample in an unused sample well. The chip was vortexed with an IKA vortexer for 1 minute at 2400 rpm and then the chip was run within 5 minutes in the Agilent 2100 bioanalyzer. Here, an electrode was placed in each of the 16 wells and extracted RNA was divided based on size through electrophoresis. Results are shown in Additional files table 2 and later discussed.

qPCR for NP samples. Quantitative PCR (qPCR) of NP samples was performed (BioRad, CFX384 Real-Time System) to determine the gene expression levels for the following biomarkers listed in Additional files table 3. The relative levels of expression were will be determined by normalizing the cycle threshold (Ct) value of each target gene by the mean Ct value of four reference genes (i.e. glyceraldehyde 3-phosphate dehydrogenase (GAPDH), ribosomal protein S19 (RPS19), succinate dehydrogenase complex, subunit A, flavoprotein variant (SDHA) and hypoxanthine-quanine phosphoribosyltransferase (HPRT) [4,6].

The arrangement of the target genes for qPCR can be seen in Additional files table 4. Every gene has its own optimal temperature for qPCR. The qPCR mix was made (SYBR GREEN 408,3 µl, 100 µM Forward Primer 3,3 µl, 100 µM Reverse Primer 3,3 µl, MQ 75,1 µl and 6 µl of mix was put in the wells of a 384 wells plate. In every well 4 µl of 50x diluted cDNA was placed, then centrifuged at 1900 rpm for 1 minute and placed in PCR machine at the right temperature.

qPCR for AF samples. To be continued in a future study.

Biochemical analysis.

Papain digestion. Papain digestion solution was made according to manufacturer's instructions (3,13 g H_2NaPO_4 * 2 H_2O (21254, Boom B.V., Meppel, the Netherlands) and 0,326 g EDTA (100944, Merck Millipore, Amsterdam, the Netherlands) adjusted to pH 6,0 and 1,57 mg cysteine HCl (C7880, Sigma-Aldrich, Saint Louis, USA) and 250 µg papine (P3125, Sigma-Aldrich, Saint Louis, USA)) and was added to every sample and incubated overnight at 60 °C.

Collagen content. The collagen content was measured using a hydroxyproline (HYP) assay according to the method of Neuman & Logan (1950) [26]. 4-hydroxyproline is a non-proteinogenic amino acid and a major component of collagen. It stabilizes the 3D-structure of collagen and because it is largely restricted to collagen the measured levels can be used as an indicator of the collagen amount [26]. The papain digested samples were freeze dried and hydrolysed overnight at 108 °C in 4M NaOH (106462, Merck Millipore, Amsterdam, The Netherlands). Later the samples were centrifuged (at 14000x g for 15 seconds) and incubated with Chloramin-T reagent (C9887, Merck Millipore, Amsterdam, The Netherlands) and placed on shaker for 20 minutes at 170 rpm. Then freshly prepared dimethylaminobenzoaldehyde (DMBA) reagent (3058, Merck Millipore, Amsterdam, The Netherlands) was added and samples were incubated for 20 minutes at 60 °C. A microplate reader was used to determine the absorbance (570nm). A standard line was made with hydroxyproline (104506.0010 Merck Millipore, Amsterdam, The Netherlands). Because 13,5% of collagen is composed of hydroxyproline, the amount of hydroxyproline was multiplied by 7,5 to calculate the collagen content [26].

GAG content. An 1,9-dimethylmethylene blue (DMMB) assay was used to quantify the GAG content of the samples according to the method of Farndale et al. (1982) [27]. The DMMB assay is the most commonly used method to estimate the amount of sulphated GAG in cell culture samples. The assay is based on a colour shift after the DMMB dye forms complexes with negatively charged sulphated GAG. This shift can be observed by measuring the differences in absorbance (540/595 nm) immediately after DMMB was added using a microplate reader. First, the DMMB staining solution was prepared one day

before use by adding 16 mg of DMMB (341088, Sigma-Aldrich, Saint Louis, USA) to 5 ml 100% ethanol and incubate on roller bench for 2-16 hours. The final solution was prepared by adding 2,37 g NaCl and 3,04 g glycine to 1L distilled water and setting the pH at 3.0, where after the 5 ml DMMB in ethanol was added. The DMMB staining solution was kept in the dark and stored at 4 °C. To prepare the PBS-EDTA solution 5,68 g 0,04 M Na_2HPO_4, 8,28 g 0,06 M H_2NaPO_4*2 H_2O and 3,72 g 0,01 M Na_2EDTA*2 H_2O was added to 1L distilled water. Chondroitin sulphate C (0,5 mg/ml (C4384, Sigma-Aldrich, Saint Louis, USA)) was diluted 1:50 in PBS-EDTA, to make the standard dilution.

A multichannel pipette was used to pipette 100 µl of standard dilution in duplicate in a 96-wells plate. The samples (10µl) were each diluted 1:10 in 90 µl PBS-EDTA and pipetted in duplicate in the 96-wells plate. Immediately after adding 200 µl of the DMMB dye, the samples were processed at room temperature. Measuring of the color shift was set at spectrums of 540 and 595 nm and was conducted by using a microplate reader [24,27].

DNA content. The DNA content of the samples was determined using a Qubit dsDNA High Sensitivity Assay Kit (Q32851, Invitrogen, Paisley, UK) according to manufacturer's instructions. The NP samples were diluted 1:40 and most of the AF samples were diluted 1:67. DNA content was used to normalize total GAG and total collagen content to cel content in the samples.

Statistical Analysis.

Due to unexpected low outcome of the qPCR there was no further statistical analyses and evaluation for gene expression.

For the results of the biochemical analyses, data were first arranged and averages were determined in Windows Excel. The two samples of dog 7345 that were mingled (L5-L6 and L6-L7) were not further evaluated, just as the samples with TAA LD and TAA HD. This left 41 samples for statistical analysis (empty PEAMs n=6; CXB LD n=5; CXB HD n=6; untreated n=24). Statistical analyses were performed using IBM SPSS statistics 22. The data were examined for normal distribution with a Shapiro Wilks test and if data did not approximate a normal distribution a log transformation was performed. If data were still non-normally distributed, then a nonparametric Kruskal-Wallis and Mann-Whitney U test were performed to determine differences between conditions. For the normal distributed data ANOVAs were used. A *Benjamini & Hochberg False Discovery Rate post-hoc test* was performed for every test [34]. An adjusted p-value of <0,05 after correction for multiple testing was considered as a significant result. Statistical analyses were performed for the NP samples and for the AF samples.

Results

qPCR for NP samples. Due to very low and inappropriate responses from the qPCR, the outcomes were not further analysed during this study.

Biochemical Analysis NP samples. Original data were not normal distributed and so a log transformation was performed that did approximate a normal distribution. ANOVAs were used for further analysis of the data. To quantify the content of collagen and GAG present in the IVDs, the concentration of GAG and collagen was determined and corrected for DNA. This gives insight into the regenerative effect of celecoxib on biochemical contents of degenerated IVDs per cell.

DNA content

The DNA content per condition was determined and shown in figure 5. There were no significant differences found between conditions for DNA content (p=0,814).

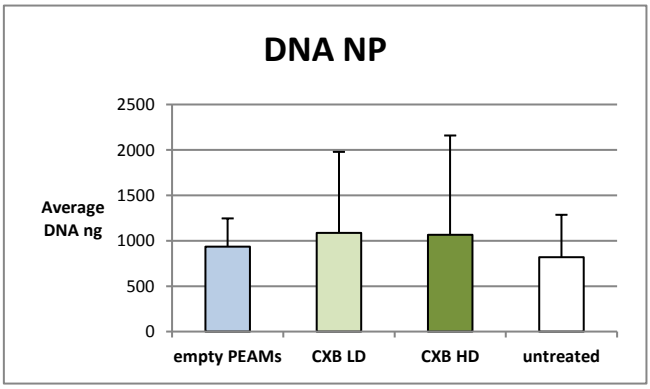

Fig. 5. DNA content per condition for the NP samples. No significant differences were found between conditions. NP = nucleus pulposus, PEAMs = polyester amide polymer microspheres, CXB LD = celecoxib low dose, CXB HD = celecoxib high dose.

Effect of different doses of celecoxib on GAG content.

Total GAG content per condition was determined and shown in figure 6. There was a significant difference between conditions (p=0,046). More specifically, GAG content in µg in empty PEAMs was significantly lower than in the samples treated with a low dose celecoxib (p=0,023) and a high dose celecoxib (p=0,044) as can be seen in figure 6 left. When corrected for DNA content in ng there were no significant differences between conditions (figure 6 right, p=0,384).

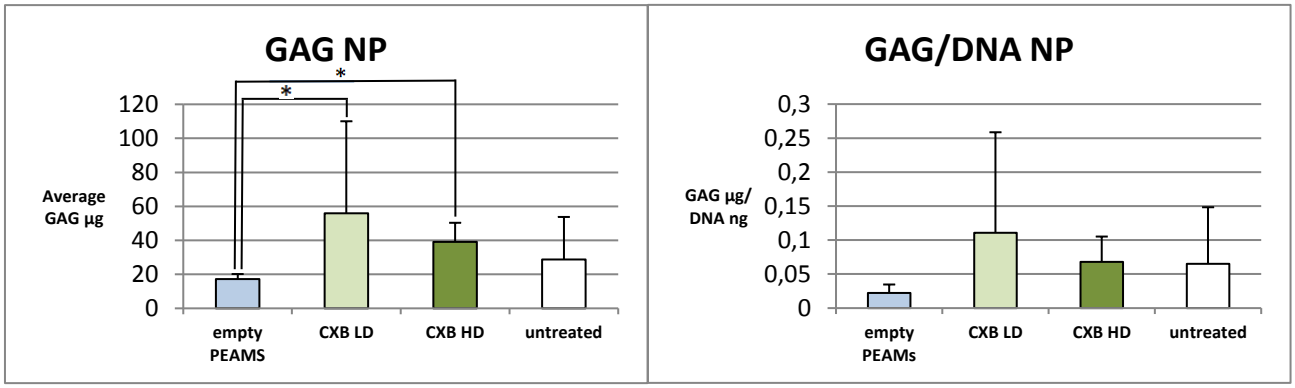

Fig. 6. Total GAG content and GAG/DNA content in the NP samples. **Left:** Significant differences between empty PEAMs and celecoxib LD (p=0,023) and celecoxib HD (p=0,044) were seen for total GAG content. **Right:** No significant differences between conditions were seen for GAG/DNA in the NP samples (p=0,384). GAG = glycosaminoglycans, NP = nucleus pulposus, PEAMs = polyester amide polymer microspheres, CXB LD = celecoxib low dose, CXB HD = celecoxib high dose.

Effect of different doses of celecoxib on collagen content.

Total collagen content per condition was determined and shown in figure 7. There was a significant difference between groups for total collagen content (p=0,014). Specifically, when distinguished between conditions, collagen content in µg in empty PEAMs was significantly lower than in the samples with low dose celecoxib (p=0,012) and high dose celecoxib (p=0,022) as can be seen in figure 7 left. Also, significant results were found between the untreated condition and low dose celecoxib (p=0.026). When corrected for DNA content in ng there was no significant difference between groups (figure 7 right, p=0,404).

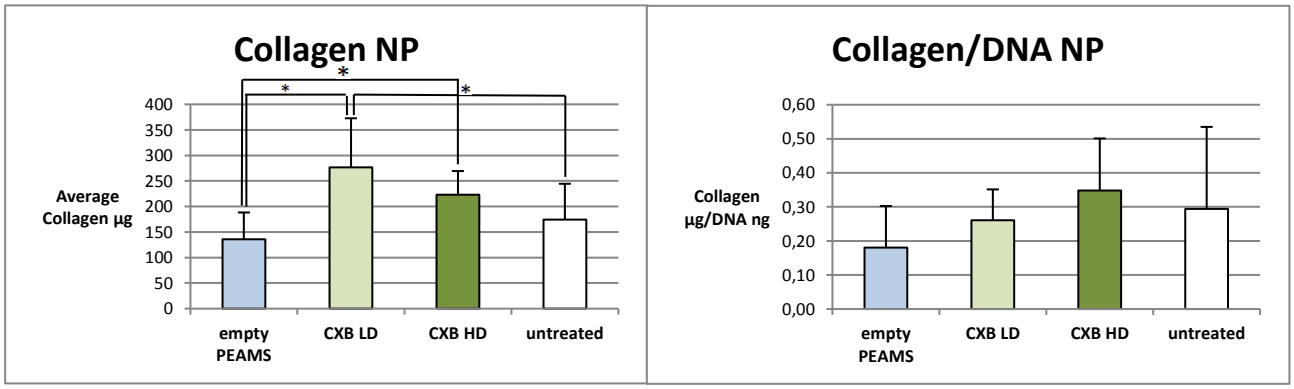

Fig. 7. Total collagen content and collagen/DNA content in the NP samples. **Left.** Significant differences between empty PEAMs and celecoxib LD (p=0,012) and celecoxib HD (p=0,022) were seen for total collagen content and between untreated and celecoxib LD (p=0,026). **Right.** No significant differences between conditions were seen for collagen/DNA in the NP samples (p=0,404). NP = nucleus pulposus, PEAMs = polyester amide polymer microspheres, CXB LD = celecoxib low dose, CXB HD = celecoxib high dose.

Biochemical Analysis AF. Original data were not normal distributed and so a log transformation was performed, but that did not approximate normal distribution for all variables. A nonparametric Kruskal-Wallis test and Mann-Whitney U test were performed.

DNA content.

The DNA content was determined and shown in figure 8. No significant differences were found between conditions for the AF samples (p=0,528).

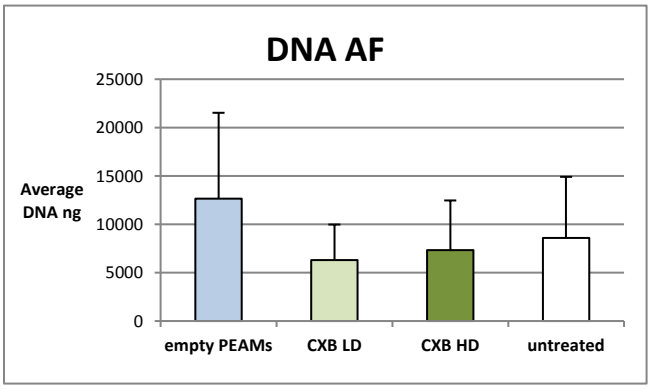

Fig. 8. DNA content per condition for the AF samples. No significant differences were found between conditions (p=0,529). AF = annulus fibrosus, PEAMs = polyester amide polymer microspheres, CXB LD = celecoxib low dose, CXB HD = celecoxib high dose.

Effect of different doses of celecoxib on GAG content.

Total GAG content per condition was determined and shown in figure 9. There was a slight tendency towards significance between groups for total GAG content (p=0,069). When examined more specifically and distinguished between conditions, GAG content in µg in empty PEAMs showed a tendency towards significance compared with high dose celecoxib (p=0,074). A significant result was found between untreated and high dose celecoxib (p=0,043) as can be seen in figure 9 left. When corrected for DNA content in ng there was no significant difference between groups (figure 9 right, p=0,198).

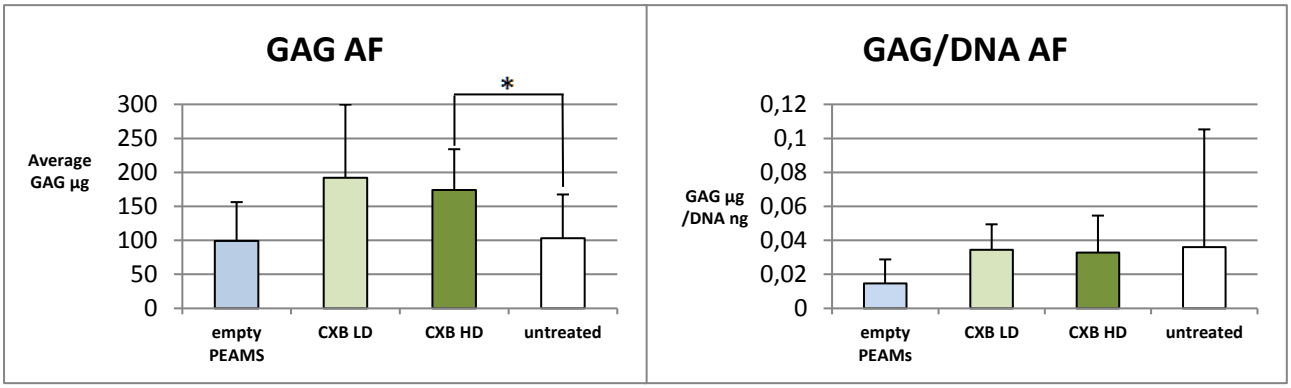

Fig. 9. Total GAG content and GAG/DNA content in the AF samples. **Left.** A slight tendency towards significant results was seen for total GAG (p=0,069), more closely examined there was a significant difference between empty PEAMs and celecoxib HD (p=0,037). **Right.** No significant differences between conditions were seen for GAG/DNA in the AF samples (p=0,198). GAG = glycosaminoglycans, AF = annulus fibrosus, PEAMs = polyester amide polymer microspheres, CXB LD = celecoxib low dose, CXB HD = celecoxib high dose.

Effect of different doses of celecoxib on collagen content.

Total collagen content per condition for the AF samples was determined and shown in figure 10. There was no significant difference between groups for total collagen content (figure 10 left, p=0,210). Furthermore, when corrected for DNA content in ng there was no significant difference between groups either (figure 10 right, p=0,295)

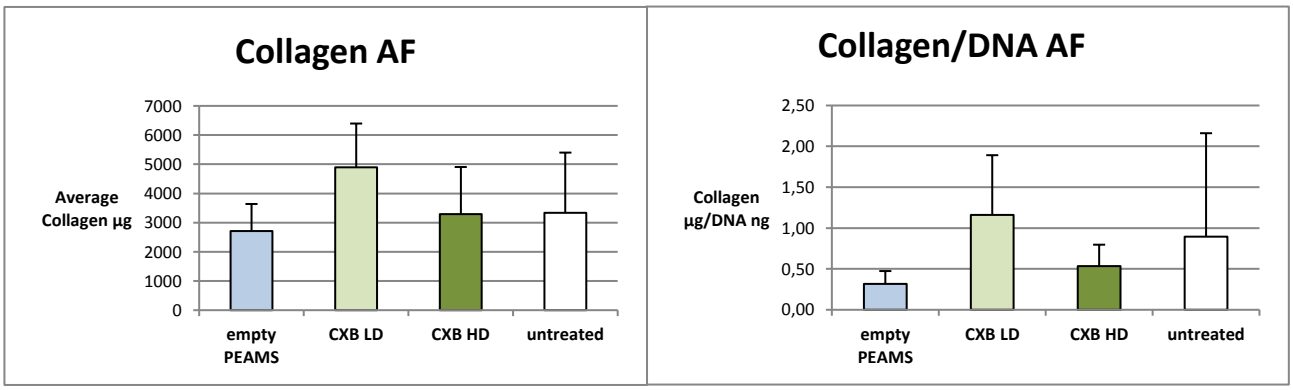

Fig. 10. Total collagen content and collagen/DNA content in the AF samples. **Left.** No significant differences were found between groups for total collagen content (p=0,210). **Right.** No significant differences between conditions was seen for collagen/DNA in the AF samples (p=0,295). AF = annulus fibrosus, PEAMs = polyester amide polymer microspheres, CXB LD = celecoxib low dose, CXB HD = celecoxib high dose.

Discussion

Based on previous studies, the effect of celecoxib on IVD degeneration seemed promising [6]. Though, not yet was the effect of slow-released celecoxib from PEAMs injected directly into the affected IVD examined in dogs. Therefore, this study focused on the effect of two doses of celecoxib gradually released from PEAMs to the degenerated IVD in a canine model. Celecoxib was selected, as this selective COX-2 inhibitor is commonly prescribed to relieve pain due to IVDD [35]. Expected would be that the higher the dose of celecoxib, the clearer the regenerative effect of celecoxib on the IVDs as would be reflected in specific gene expression and increased GAG and collagen content.

Controlled release of low dose of celecoxib resulted in an increase of GAG and collagen content in the NP samples.

Results of the NP samples showed a tendency that controlled release of a low dose celecoxib was effective in creating more GAG deposition and more collagen synthesis compared with empty PEAMs then when empty PEAMs were compared with a high dose of celecoxib. This effect could have been related to the working mechanism of celecoxib as a COX-2 inhibitor. In the study done by Liu *et al.* (2003), the assumption was made that when a higher concentration (range 10-50 μM) was adminstered there was more effect seen in somatic cells of mice [31]. This dose-dependent effect could be the expected positive effect, thus more regenerative due to the anti-inflammatory properties of celecoxib leading to more GAG and collagen, but the dose-dependent effect could also be less positive than expected [31]. This less positive dose-dependent side effect of celecoxib could be explained when another application of selective COX-2 inhibitors is incorporated and discussed [31]. Selective COX-2 inhibitors are gaining interest as a cancer treatment due to beneficial clinical characteristics, like the inhibition of cell proliferation and angiogenesis, and the induction of differentiation, maturation and apoptosis in various cancer cells [31,32,33]. For example, 80% of colon carcinomas showed an enhanced COX-2 expression and excessive prostaglandin production compared with healthy tissue, making selective COX-2 inhibitors an excellent choice of treatment [33]. Also, assumptions were made that there is a dose-dependent effect of celecoxib on cell cycle arrest in three different kinds of human colon cancer cell lines [33]. However, not much is known about this working mechanism. Celecoxib and other NSAIDs have an inhibitory effect on the synthesis of prostaglandins, which are not only important for inflammation but also essential for normal cell homeostasis [19,31,33]. It could be that a high dose of celecoxib may exhibit the same dose-dependent effect when injected into degenerated IVDs, thereby causing less GAG deposition and less collagen synthesis compared with a lower dose of celecoxib due to the effect on cell homeostasis. However, a clear comparison between studies is difficult, because when used as a cancer treatment celecoxib is not locally injected like in degenerated IVDs, thus comparison of specific concentrations and their effects at the site of interest is not possible.

GAG and collagen corrected for DNA did not result in a significant effect of celecoxib.

Only significant effects of celecoxib on GAG and collagen content were found when data were not corrected for DNA. The correction for DNA was made to quantify the extracellular GAG and collagen content per cell and to further evaluate than only the overall amount of GAG and collagen. The intracellular DNA content itself showed little variation between conditions for the NP samples, but in the AF samples DNA content was even lower in the celecoxib conditions compared to the controls. As mentioned before, celecoxib is known to have an inhibitory effect on cell proliferation and it disturbs cell homeostasis, what could explain the lower cell content in both celecoxib conditions in the AF samples [31,33]. More informative results would be expected if the tissue was weighted prior to cutting of the cryosections to make it able to correct the results for dry weight [6].

Differences in biochemical composition between NP and AF samples.

Although both tissues play a different role during axial movement and compression of the spine, they are both made up from mainly proteoglycans, collagen type II and elastin fibres [2,17,37]. Nevertheless, samples from NP tissue showed more and different significant results for biochemical composition compared with samples from the AF tissue. This deviation may be explained when the biochemical composition is further evaluated [37,38]. The NP is made up of mainly GAGs and a small portion of collagen type II, ratio 28:1, whereas in the AF there are far less GAGs but more collagen type I in the outer layers. The type of small interstitial proteoglycan is also different with decorin being more abundant in the AF and biglycan in the NP [39]. In the study done by Sakai *et al.* (2009)[37] they examined gene expression of specific molecules in healthy rats to identify biochemical composition of NP and AF. Some molecules showed a log-ratio of 3 or more when NP was compared with AF, like CK18, A2M, DSC2, Wnt inhibitory factor-1, desmoplakin, UDP-glucose dehydrogenase, carbonic anhydrase II and ADAMTS 10 [37]. For these molecules a big difference in gene expression was seen between NP and AF, leading to a different composition and characteristics of the ECM in NP compared to AF [31]. These differences at the beginning could lead to different results for biochemical content at the end.

Evaluation of collagen content showed differences in NP tissue, but not in AF tissue. This might be explained by the heterogeneous content of collagen in the AF. The outer layers of the AF contain mostly collagen type I, whereas the inner layers reaching the TZ contain predominantly collagen type II [2,37]. Samples were taken from the whole AF and made no distinction between the inner and outer layers. Because during IVDD, the collagen type II fibres are denatured and synthesis is decreased together with an increase of synthesis of collagen type I fibres there will be less variation in the overall content of collagen as both types are replacing each other [2,17,37]. In this study, the HYP assay was used to determine the content of collagen. However, the outcome of the HYP assay represents all types of collagen present in the sample without discriminating between the types of collagen and between procollagen, mature collagen and collagen degradation products [26]. To discriminate between collagen types I and II immunohistochemistry (IHC) is commonly performed [24]. IHC uses antigen-antibody complexes to make the collagen visible under microscope [24], a technique that could be useful in this study to define the content of each type of collagen.

Limitations of the study.

Donor dogs. The first limitation of this study is that the dogs used were not patients suffering from degenerative IVD conditions with associated pain symptoms. However, no real patients can be included, before the safety is extensively examined in a lare animal model like this study, making the use of donor dogs unavoidable. The degeneration was artificially induced according to the needle aspiration method of Hiyama *et al.* (2008) [23]. This method is known as the reference technique for IVDD induction [23,30]. A histological comparison between this method and induction through a laser approach in rabbits led to the assumption that IVDD after the laser approach was more progressive, less deleterious to the extracellular medium of the NP and more similar to the degeneration obtained during normal aging [30]. Further, needle aspiration is an acute process and it probably does not reflect the complexity of early degeneration, like progressive dehydration of the nucleus pulposus [30]. The less destructive laser approach is more likely to mimic these early and less radical changes and therefore it may be a better induction method for IVDD than needle aspiration.

Second, one of the donor dogs had 8 instead of 7 lumbar discs, only to be found out during MR imagining after intradiscal injection. During induction and injection this was not accounted for and led to a different induction and injection protocol compared with other donor dogs, eventually creating a disc (L5-L6) with induction but no treatment and a disc (L6-L7) without induction but with injection of celecoxib low dose. Both discs were not taken into account for the results and statistical analysis. This resulted in a different sample size per condition, with the low dose celecoxib condition consisting of 5 instead of 6 samples, as were the conditions high dose celecoxib and empty PEAMs.

Quantitative PCR. The results of the qPCR were disappointing, but may be explained. For proper qPCR samples must contain a certain amount of RNA after isolation. Normally, IVD tissue does not possess much RNA, so a quantitative RNA assay was done after isolation to determine the actual content of RNA. Results showed a sufficient content of RNA, but this also contained small RNAs that were not transcribed into cDNA and analysed in the qPCR. This means that RNA quantification might have measured enough RNA, but that it still led to inappropriate qPCR responses. Therefore, a bioanalysis was performed on 11 randomly chosen NP samples to measure again the RNA content, but also the RNA Integrity Number (RIN) which reflects a selection of features that contribute information about the integrity of the RNA [36]. Possible values of RIN range from 1 to 10, with 1 meaning RNA is completely degraded into small parts and 10 meaning RNA is most valuable and intact [36]. RIN values of 7 or more are accepted as valid for further analysis [36]. The RIN values of the NP samples ranged from 2,20 to 3,20 leading to the conclusion that RNA in the samples was very small in size and degraded and not valid for further transcribing into cDNA and eventually qPCR analysis. This is the main and most likely explanation for the disappointing results of the qPCR. There are many explanations for the low RIN values and degradation of RNA, like improper storage on ice of the samples. Also, there might be too little tissue available for RNA isolation, because of all the tests that were conducted or tissue loss may have occurred during cutting for MSI.

Also, the results of the qPCR may be due to technical faults.

Future research.

Some limitations of this study might be improved and implied in future research. Instead of using donor dogs, it would be more valuable to use actually patients suffering from IVDD. When the results of this study are combined with the expected results from IHC and MRI, more conclusions can be made about safety of the treatment. If results are positive, then celecoxib loaded PEAMs could be injected in a larger group of real patients to test clinical effectiveness by determing the analgetic effect. If not, the protocol and method of induction and injection has to be optimalised and tested again in a conditioned setting. Optimalisation might be induction of IVDD with the laser approach, a longer period between induction and injection to let the degeneration take place for a longer period of time or more dogs and thus more IVDs to increase statistical power. However, to get a substanial increse of statistical power a lot more dogs have to be part of the study, which is ethically undesirable. Furthermore, for future research it might be valuable to focus on a specific field of interest instead of cutting the IVDs multiple times for different laboratory experiments. This may improve the RNA content of the samples and therefore increase the chance of useful results from the qPCR. As always, samples should be treated carefully and placed on ice every time. An IHC for collagen can be an addition to the protocol to distinguish between types.

This study showed a tendency that a low dose of celecoxib is already effective, however more results have to be acquired and evaluated before an optimal concentration can be determined. This study is still ongoing and if results are positive for MSI, MRI imaging and IHC than the treatment of celecoxib loaded PEAMs can be further applied to canine patients with IVDD.

Conclusion

Overall, the results of this study so far show a tendency that a low dose of celecoxib might be already effective and led to equal or even higher concentrations of GAG and collagen compared with the high dose celecoxib. However, when both conditions were compared, no significant differences were found. For almost every variable the two control conditions (empty PEAMs and untreated) scored lower compared to both concentrations of celecoxib, concluding that there might be a positive regenerative effect of celecoxib on GAG and collagen in both NP and AF samples independent of concentration of celecoxib. Furtermore, results show no negative effect of celecoxib on biochemical content, making it a safe therapy for IVDD. Results of other analyses have to be taken into account before more general conclusions about celecoxib can be made.

For the NP samples, the significant results found for collagen content between empty PEAMs and low dose of celecoxib and between empty PEAMs and high dose of celecoxib may lead to the conclusion that celecoxib has a positive effect on collagen synthesis in degenerated IVDs. Also, the significant difference in collagen content between the untreated condition and low dose of celecoxib may arise to the conclusion that celecoxib does not have a regenerative effect when injected into IVDs that were not induced. Next, for the GAG content the significant results between empty PEAMs and both concentrations of celecoxib may lead to the conclusion that celecoxib leads to more GAG deposition in degenerated IVDs independent of the dose of celecoxib.

For the AF samples, there was only a significant result found for total GAG content between the conditions untreated and high dose of celecoxib. This led to the conclusion that only a high dose of celecoxib might give more GAG deposition compared with untreated IVDs.

References

1. Bergknut N, Rutges JPHJ, Kranenburg HJC, Smolders LA, Hagman R, Smidt HJ, Lagerstedt AS, Penning LC, Voorhout G, Hazewinkel HAW, Grinwis GCM, Creemers LB, Meij BP & Dhert WJA (2012). The dog as an Animal Model for Intervertebral Disc Degeneration?, SPINE, vol 37, n 5, p 351-358.
2. Bergknut N, Smolders LA, Grinwis GCM, Hagman R, Lagerstedt AS, Hazewinkel HAW, Tryfonidou MA & Meij BP (2013). Intervertebral disc degeneration in the dog. Part 1: Anatomy and physiology of the intervertebral disc and characteristics of intervertebral disc degeneration, The Veterinary Journal, 195.3, p 282-291.
3. Parker HG, VonHoldt BM, Quignon P, Margulies EH, Shao S, Mosher DS, Spady TC, Elkahloun A, Cargill M, Jones PG, Maslen CL, Acland GM, Sutter NB, Kuroki K, Bustamante CG, Wayne RK & Ostrander EA (2009). An Expressed Fgf4 Retrogene Is Associated with Breed-Defining Chondrodysplasia in Domestic Dogs, Science, 325, issue 5943, p 995-998.
4. Willems N, Mihov G, Grinwis GCM, van Dijk M, Schumann D, Bos C, Strijkers GJ, Dhert WJA, Meij BP, Creemers LB & Tryfonidou MA (2015). Safety of intradiscal injection and biocompatibility of polyester amide microspheres in a canine model predisposed to intervertebral disc degeneration, Journal of Biomedical Materials Research Part B, p 1- 8.
5. Kranenburg HJC, Grinwis GCM, Bergknut N, Gahrmann N, Voorhout F, Hazewinkel HAW & Meij BP (2013). Intervertebral disc degeneration in dogs – part 2: comparison of clinical, magnetic resonance imaging, and histological findings in 74 surgically treated dogs, The Veterinary Journal, 195, p 164-171.
6. Willems N, Yang HY, Langelaan MLP, Tellegen AR, Grinwis GCM, Kranenburg, HJC, Riemers FM, Plomp SGM, Craenmehr EGM, Dhert WJA, Papen-Botterhuis NE, Meij BP, Creemers LB & Tryfonidou MA (2015). Biocompatibility and intradiscal application of a thermoreversible celecoxib-loaded poly-N-isopropylacrylamide MgFe-layered double hydroxide hydrogel in a canine model. Arthritis Research & Therapy, 17, 214-229.
7. Gruber HE, Ingram J, Hanley EN Jr (2002). An improved staining method for intervertebral disc tissue, Biotech Histochem, 77, 81-83.
8. Kepler CK, Ponnappan RK, Tannoury CA, Risbud MV & Anderson DG (2013). The molecular basis of intervertebral disc degeneration, The Spine Journal, 13, 318-330.
9. Bagci, E. Z., et al. "Bistability in apoptosis: roles of bax, bcl-2, and mitochondrial permeability transition pores." Biophysical journal 90.5 (2006): 1546-1559.
10. Mern DS, Beierfuss A, Fontana J, Thome C & Hegewald AA (2014). Imbalanced Protein Expression Patterns of Anabolic, Catabolic, Anti-Catabolic and Inflammatory Cytokines in Degenerative Cervical Disc Cells: New Indications for Gene Therapeutic Treatments of Cervical Disc Diseases. PLOS, volume 9, issue 5 p 1-11.
11. Ohtori S, Inoue G, Miyagi M & Takahashi K (2015). Pathomechanisms of discogenic low back pain in humans and animal models. The Spine Journal, vol 15 p 1347-1355.
12. www.cbg-med.nl. Instruction manual of Celecoxib.
13. Sareddy GR, Kesanakurti D, Kirti PB, Babu PP (2013). Nonsteroidal Anti-inflammatory Drugs Diclofenac and Celecoxib Attenuates Wnt/b-Catenin/Tcf Signaling Pathway in Human Glioblastoma Cells. Neurochemical Research, vol 38 p 2313–2322.
14. Liu Y, Fu S, Rahaman MN, Mao JJ, Bal BS (2015). Native nucleus pulposus tissue matrix promotes notochordal differentiation of human induced pluripotent stem cells with potential for treating intervertebral disc degeneration. Journal of Biomedical Materials Research Part A, vol103 p 1053–1059.
15. Willems N, Tellegen AR, Bergknut N, Creemers LB, Wolfswinkel J, Freudigmann C, Benz K, Grinwis GCM, Tryfonidou MA, Meij BP (2016). Inflammatory profiles in canine intervertebral disc degeneration. BMC Veterinary Research, vol 12, 10 p 1-12.
16. Bertolini A, Ottani A & Sandrini M (2002). Selective COX-2 inhibitors and dual acting anti-inflammatory drugs: critical remarks. Current Medical Chemistry, 2002 May;9(10):1033-43.

17. Bach FC, Willems N, Penning LC, Ito K, Meij BP, Tryfonidou MA (2014). Potential regenerative treatment strategies for intervertebral disc degeneration in dogs. BMC Veterinary Research, vol 4, 10:3 p 1-12.
18. Kyöstilä K, Lappalainen AK & Lohi h (2013). Canine Chondrodysplasia Caused by a Truncating Mutation in Collagen-Binding Integrin Alpha Subunit 10, PLoS ONE vol 8, issue 9: e75621.
19. Shen G (2005). The role of type X collagen in facilitating and regulating endochondral ossification of articular cartilage. Orthodontics & Craniofacial Research, vol 8 p 11-17.
20. Sharan AD, Tang SY & Vaccaro AR (2013). Basis science of Spinal Diseases. Jaypee Brothers Medical Publishers Ltd. Chapter 6: Animal models for disc degeneration (Kranenburg HC, Ito K, Tryfonidou MA, Smolders LA, Bergknut N, Oner FC, Hazewinkel HAW, Dhert WJA & Meij BP). p 44
21. Scheller J, Chalaris A, Schmidt-Arras D, Rose-John S (2011). The pro- and anti-inflammatory properties of cytokine interleukin-6. Biochimica et Biophysica Acta, vol 1813, p 878-888.
22. Bergknut N (2010). Intervertebral Disc Degeneration in Dogs. Doctoral Thesis no. 2010:91, p 1-180.
23. Hiyama A, Mochida J, Iwashina T, Omi H, Watanabe T, Serigano K, Tamura F & Sakai D (2008). Transplantation of mesenchymal stem cells in a canine disc degeneration model. Journal of orthopaedic research, p 589-601.
24. Bach FC, de Vries SAH, Krouwels A, Creemers LB, Ito K, Meij BP & Tryfonidou MA (2015). The species-specific regenerative effects of notochordal cell-conditioned medium on chondrocyte-like cells derived from degenerated human intervertebral discs. European cells and materials, vol 30 p 132-147.
25. Willems N, Bach FC, Plomp SGM, van Rijen MHP, Wolfswinkel J, Grinwis GCM, Bos C, Strijkers GJ, Dhert WJA, Meij BP, Creemers LB & Tryfonidou MA (2015). Intradiscal application of rhBMP-7 does not induce regeneration in a canine model of spontaneous intervertebral disc degeneration. Arhtritis Research & Therapy, vol 17, p 137-
26. Neuman RE & Logan MA (1950). The determination of hydroxyproline. Journal of Biological Chemistry, vol 184, p: 299-306.
27. Farndale RW, Sayers CA & Barrett AJ (1982). A direct spectrophotometric microassay for sulfated glycosaminoglycans in cartilage cultures. Connective Tissue Research, vol 9 (4), p 247-248.
28. Brisson BA (2010). Intervertebral disc disease in dogs. Veterinary Clinics of North America: Small Animal Practice, vol 40, p 829-858.
29. Yurube T, Hirata H, Kakutani K, Maeno K, Takada T, Zhang Z, Takayama K, Matsushita T, Kuroda R, Kurosaka M & Nishida K (2014). Notochordal cell disappearance and modes of apoptotic cell death in a rat tail statis compression-induced disc degeneration model. Arthritis Research & Therapy, vol 16: R31.
30. Lucas O, Hamel O, Blanchais A, Lesoeur J, Abadie J, Fellah BH, Fusellier M, Gauthier O, Bord E, Grimandi G, Vinatier C, Guicheux J & Clouet J (2012). Laser-treated nucleus pulposus as an innovative model of intervertebral disc degeneration. Experimental Biology and Medicine, vol 237, p 1359–1367.
31. Liu W, Chen Y, Wang W, Keng P, Finkelstein J, Hu D, Liang L, Guo M, Fenton B, Okunieff P & Ding I (2003). Combination of radiation and celebrex (celecoxib) reduce mammary and lung tumor growth. American Journal of Clinical Oncology (CCT), vol 26.4 supplement 2, p 103–109.
32. Zhou G, Shi X, Ren K, Fan GT, Wu SJ & Zhao JN (2015). Celecoxib inhibits cell growth and modulates the expression of matrix metalloproteinases in human osteosarcoma MG-63 cell line. European Review for Medical and Pharmacological Sciences, vol 19, p 4087-4094.
33. Grösch S, Tegeder I, Niederberger E, Bräutigam L and Geisslinger G (2001). COX-2 independent induction of cell cycle arrest and apoptosis in colon cancer cells by the selective COX-2 inhibitor celecoxib. The FASEB Journal, p 1-23.

34. DeCoster, J. (2004). Data Analysis in SPSS. Retrieved from http://www.stat-help.com/notes.html
35. Sun TW, Wu ZH & Weng XS (2015). Celecoxib can suppress expression of genes associated with PGE2 pathway in chondrocytes under inflammatory conditions. International Journal of Clinical and Experimental Medicine, vol 8, issue 7, p: 10902-10910
36. Schroeder A, Mueller O, Stocker S, Salowsky R, Leiber M, Gassmann M, Lightfoot S, Menzel W, Granzow M & Ragg T (2006). The RIN: a RNA integrity number for assigning integrity values to RNA measurements. BMC Molecular Biology, vol 7, issue 3, p 1-14.
37. Sakai D, Nakai T, Mochida J, Alini M & Grad S (2009). Differential phenotype of intervertebral disc cells. Spine, vol 34, issue 14, p 1448-1456.
38. Rutges J, Creemers LB, Dhert W, Milz S, Sakai D, Mochida J, Alini M & Grad S (2010). Variations in gene and protein expression in human nucleus pulposus in comparison with annulus fibrosus and cartilage cells: potential associations with aging and degeneration. Osteoarthritis and Cartilage, vol 18, p 416-423.
39. Pattappa G, Li Z, Peroglio M, Wismer N, Alini M & Grad S (2012). Diversity of intervertebral disc cells: phenotype and function. Journal of Anatomy, vol 221, p 480-496.
40. Andrés-Guerrero V, Zong M, Ramsay E, Rojas B, Sarkhel S, Gallego B, de Hoz R, Ramírez AI, Salazar JJ, Triviño A, Ramírez JM, del Amo EM, Cameron N, de-las-Heras B, Urtti A, Mihov G, Dias A & Herrero-Vanrell R (2015). Novel biodegradable polyesteramide microspheres for controlled drug delivery in Ophthalmology. Journal of Controlled Release, vol 211, p 105-117.

Additional files

Results of the Aligent 6000 Pico Bioanalyzer:

Sample	1	2	3	4	5	6
RIN	3,20	2,20	2,30	2,50	2,40	2,30
Pg/µl	1269,37	2552,025	7469,616	1412,574	4142,008	1532,154

Sample	7	8	9	10	11	L
RIN	2,90	2,40	2,50	2,20	2,20	
Pg/µl	15824,68	4244,128	1904,656	729,4703	2656,47	1000

Table 1. Qualitative results from the Aligent 6000 Pico Bioanalyzer performed on 11 randomly chosen NP samples and a reference ladder. RIN = RNA Integrity Number, a subjective value which qualify the RNA content, 1 = most degraded RNA and 10 = most intact RNA [36].

Results of Qubit RNA fluorometer assay:

Sample nr	NP		Condition	RNA ng/ml	Corrected for dilution stock RNA ng/ml	ng per 15 ul for cDNA
1	dog 7269	T12-T13	empty PEAMS	118	2360	35,4
2		T13-L1	untreated	253	5060	75,9
3		L1-L2	TAA LD	220	8800	132
4		L2-L3	untreated	184	3680	55,2
5		L3-L4	TAA LD	468	9360	140,4
6		L4-L5	untreated	308	6160	92,4
7		L5-L6	TAA HD	84	3360	50,4
8		L6-L7	untreated	356	7120	106,8
9		L7-S1	TAA HD	225	9000	135
10	2645	T12-T13	empty PEAMS	369	7380	110,7
11		T13-L1	untreated	269	5380	80,7
12		L1-L2	TAA LD	257	5140	77,1
13		L2-L3	untreated	252	5040	75,6
14		L3-L4	TAA HD	205	8200	123
15		L4-L5	untreated	477	9540	143,1
16		L5-L6	TAA HD	285	5700	85,5
17		L6-L7	untreated	97	3880	58,2
18		L7-S1	TAA LD	364	7280	109,2
19	5466	T12-T13	empty PEAMS	510	10200	153
20		T13-L1	untreated	328	6560	98,4
21		L1-L2	TAA HD	410	8200	123

22		L2-L3	untreated	128	2560	38,4
23		L3-L4	TAA LD	252	5040	75,6
24		L4-L5	untreated	418	8360	125,4
25		L5-L6	TAA HD	297	5940	89,1
26		L6-L7	untreated	179	7160	107,4
27		L7-S1	TAA LD	256	5120	76,8
28	7345	T12-T13	empty PEAMS	191	3820	57,3
29		T13-L1	untreated	560	11200	168
30		L1-L2	CXB HD	217	4340	65,1
31		L2-L3	untreated	132	5280	79,2
32		L3-L4	CXB LD	273	5460	81,9
33		L4-L5	untreated	457	18280	274,2
34		L5-L6	none	254	10160	152,4
35		L6-L7	CXB LD	182	3640	54,6
36		L7-L8	untreated	142	5680	85,2
37		L8-S1	CXB HD	395	7900	118,5
38	7362	T12-T13	empty PEAMs	104	4160	62,4
39		T13-L1	untreated	183	3660	54,9
40		L1-L2	CXB HD	133	2660	39,9
41		L2-L3	untreated	401	8020	120,3
42		L3-L4	CXB LD	238	4760	71,4
43		L4-L5	untreated	159	6360	95,4
44		L5-L6	CXB HD	51,7	2068	31,02
45		L6-L7	untreated	379	15160	227,4
46		L7-S1	CXB LD	213	4260	63,9
47	9054	T12-T13	empty PEAMs	152	6080	91,2
48		T13-L1	untreated	339	6780	101,7
49		L1-L2	CXB HD	317	12680	190,2
50		L2-L3	untreated	321	6420	96,3
51		L3-L4	CXB HD	311	12440	186,6
52		L4-L5	untreated	257	5140	77,1
53		L5-L6	CXB LD	254	5080	76,2
54		L6-L7	untreated	285	5700	85,5
55		L7-S1	CXB LD	428	8560	128,4

Table 2. Results of Qubit RNA fluorometer assay.

List of biomarkers for quantitative PCR for the NP samples:

ECM enzymes	**anabolism**	**Name**	**field of effect**	**Ref**
ACAN		Aggrecan	Primary proteoglycan found in the IVD and crucial for normal function of the disc.	8

COL2A1	Collagen type 2	The predominant component in the ECM of the healthy NP.	8
COL1A1	Collagen type 1	The predominant component in the ECM of the healthy AF, providing strength to resist compressive load. [Col1] increases with degeneration in the NP.	8
COL10	Collagen type 10	A reliable marker for new bone formation in articular cartilage. Expression is increased with advancing degeneration, resulting in NP fibrosis and a loss of the distinct border between NP and AF.	8, 19
ECM catabolism enzymes			
ADAMTS5	A disintegrin and metallo-proteinase with thrombospondin motifs 5	An aggrecanase; catabolic enzyme of the most prominent proteoglycan in the IVD.	8
MMP 13	Matrix metallo-proteinase 13	Has a direct effect on matrix damage and indirectly through activation of collagenases.	8
MMP 2*, 9	Matrix metallo-proteinase 9	Both have a direct effect on matrix damage and indirect effect through degradation of denatured collagen.	8
MMP 3	Matrix metallo-proteinase 3	Has a direct effect on matrix damage and indirect effect through activation of stromelysin (which degrades non-collagen matrix proteins).	8
TIMP1	Tissue inhibitor of metalloproteinase 1	An anti-catabolic factor, inhibitor of MMPs.	8
Inflammation			
TNFα	Tumour necrosis factor α	Contributes to associated pain in IVD degeneration.	8
IL1B	Interleukin-1B	Pro-inflammatory cytokine, inhibitor of the production of ECM, increases production of degenerative enzymes, making IVD more sensitive for apoptosis.	8
IL6	Interleukin-6	Pro- and anti-inflammatory cytokine, known to accelerate degenerative processes like IVD degeneration through the classic signalling pathway, but can also work anti-inflammatory or regenerative by activating the process of trans-signalling in the cell.	2, 21
IL10	Interleukin-10	Pro-inflammatory cytokine, known to accelerate degenerative processes like IVD degeneration.	15
NGF*	Nerve growth factor	Associated with the ingrowth of sensory nerve fibres into the IVD causing neurogenic pain.	11
COX pathway and PGE_2 synthesis			

PTGES1	Prostaglandin E synthase 1	Enzyme producing pathological prostaglandin E_1 as found in chronic inflammatory processes.	6
PTGES2	Prostaglandin E synthase 2	Enzyme for regulatory prostaglandin E_2 homeostasis but also plays an important role in pathological processes.	6
COX1	Cyclooxygenase 1	Promotor of PGE_2 from arachidonic acid in healthy tissues for homeostasis.	6
COX2	Cyclooxygenase 2	Promotor of PGE_2 triggered by inflammatory stimuli and plays an important role in the PGE_2 production in degenerative processes.	6
Apoptosis			
BCL2	B-cell lymphoma 2	An anti-apoptotic protein which inhibits the pro-apoptotic proteins.	9
BAX	BCL-associated X	Pro-apoptotic protein leading to mitochondrial permeability.	9
Notochordal markers			
T	Brachyury	A typical notochordal protein, encoded by the notochordal marker gene T.	14
CK8	Cytokeratin-8	A keratin protein expressed in notochordal cells and therefor useful as a typical marker gene.	14
CK18	Cytokeratin-18	A keratin protein expressed in notochordal cells and therefor useful as a typical marker gene.	14
Indirect effects of CXB on Wnt signalling pathway			
AXIN2	Axin-2	A target gene, that due to CXB is reduced in expression leading to less activation of the Wnt signalling pathway.	13
c-Myc	c-Myc	A target gene, that due to CXB is reduced in expression leading to less activation of the Wnt signalling pathway.	13
CCND1	Cyclin-D1	A target gene, that due to CXB is reduced in expression leading to less activation of the Wnt signalling pathway.	13
*** At the time of writing it is uncertain if MMP2 and NGF gene expression will be taken into account due to the current lack of suitable primers.**			

Table 3. List of biomarkers for qPCR of NP samples..

Plate nr.	Gene 1	Gene 2	Gene 3	Gene 4	Temp
1	IL1B	PTGES1			68
2	T				53
3	RPS19	SDHA	c-Myc	Col2A1	61
4	BCL2	CK8	IL10	MMP9	63

5	TIMP1					66
6	Axin2	Cox2	MMP3	PTGES2		60
7	CCND1	CK18				60
8	GADPH	HPRT	BAX			58
9	Acan	Adamts5	Col1A1	Col10		61
10	IL6	MMP13	TNFa			65
11	Cox1					65

Table 4. **Arrangement of genes per plate.** During each round of qPCR four genes can be measured. The genes in red are the reference genes. In the column (Temp) the optimal temperatures are listed for qPCR. Not taken into account: MMP2 and NGF.

Titel?

Post-hoc analyses for one-way between-subjects ANOVA. A significant F statistic tells you that at least two of your means are different from each other, but does not tell you where the differences may lie. *Researchers commonly perform post-hoc analyses following a significant ANOVA to help them understand the nature of the relationship between the IV and the DV. The most commonly reported post-hoc tests are (in order from most to least liberal): LSD (Least Significant Difference test), SNK (Student-Newman-Keuls), Tukey, and Bonferroni. The more liberal a test is, the more likely it will find a significant difference between your means, but the more likely it is that this difference is actually just due to chance. 14 Although it is the most liberal, simulations have demonstrated that using LSD post-hoc analyses will not substantially increase your experimentwide error rate as long as you only perform the post-hoc analyses after you have already obtained a significant F statistic from an ANOVA. We therefore recommend this method since it is most likely to detect any differences among your groups. (*DeCoster, J. (2004). Data Analysis in SPSS. Retrieved from http://www.stat-help.com/notes.html)

Both tissues are essential for axial movement of the spine, but contain different molecules. NP is rich in proteoglycans and collagen type II, whereas AF has far less proteoglycans and both collagen type II (inner layers) and type I (outer layers). In the NP there is more biglycan and in the AF more decorin (small interstitial proteoglycans). Furthermore, Sakai et al. (2009) showed that there is 1000 times more A2M in the NP, which is an inhibitor of aggrecanases. Aggrecanases break down aggrecan, the major proteoglycan in the IVD.